総 説

Recent Advances in Synthetic Fiber Spining

Chang Dae Han*

1. Introduction

Since Nylon was first introduced into the world in 1939, the technique of spinning synthetic fibers has made considerable progress, in particular during the past decade. Not only a variety of new synthetic fibers, but also new spinning processes have been developed. It is interesting to note that, for a given fiber-forming material, different spinning techniques can sometimes produce fibers possessing markedly improved physical and/or mechanical properties. Therefore the fiber industry has put continuous efforts into modifying existing processes or developing new ones.

However, many details of spinning technique have been the carefully guarded secrets of various fiber manufactures and only, 'superficial' information of these developments is given in the numerous patents in various countries.

It has been only during the past 10~15 years that some fundamental studies of spinning technique have been reported in the literature. As some of the recent literature indicates, an understanding of fiber spinning requires a knowledge of momentum, energy and/or mass transport. In addition, knowledge of macromolecular behavior under deformation (i. e. stretching) is also necessary for understanding such complicated problems as molecular orientation under stretching, crystallization kinetics under cooling, and fiber morphology as affected by spinning conditions.

Of course the synthesis of fiber-forming material is of utmost importance. However, unless there is a criterion (or criteria) established for determining fiber spinnability, progress in synthesizing new fiber-forming materials or modifying the structure of existing materials will be very slow. A criterion of fiber spinnability should be related to the flow behavior of a fiber-forming material in the **liquid state.** Since almost all fiber-forming materials are macromolecules (i. e. polymers) a complete understanding of the flow behavior of polymeric materials (solutions and melts) requires knowledge of a separate branch of science, i. e. rheology. Since propress in the rheology of polymeric materials has been very low, one can understand why so little has been reported of such fundamental questions as relating the fiber spinnability to molecular structure, molecular weight, and the molecular weight distribution.

There are three conventional types of spinning process, commonly known as (a) melt spinning, (b) wet spinning, and (c) dry spinning. In melt spinning, the bulk polymer is melted and extruded through the spinnerette and then the liquid threadlines get solidified while passing through a cooling medium. Commerical fibers such as Nylon, polyester and polyolefin fibers are melt spun. An important requirement for a polymer to be melt spun is that the polymer should not degrade when softened upon heating. Hence a polymer which may be degradable at the desired temperature for spinning is not suitable for melt spinning. Sometimes the problem of thermal

*Professor of Chemical Engineering, Polytechnic Institute of Brooklyn, Brooklyn, New York, U. S. A. 11201.

degradation can be avoided by adding a thermal stabilizer or plasticizer. Because some plasticizers (internal type) are low molecular weight substances, they can reduce the melting point of a polymer below its thermal degradation point.

The melt spinning process has two advantages over the wet spinning process. One is that it gives a high production rate, and another is that there is no problem of solvent recovery. The high production rate is accomplished by the relatively low drag force acting on the filament while passing thruogh a cooling gas medium. For instance, the stretch rate can go as high as 1000 m/min., depending on the type of material, its rheological properties and melt temperature. Note however that the magnitude of drag force increases as the stretch rate is increased. There are some studies reported which show how one can calculate the drag force in melt spinning[1, 2]. Since the viscosity of a melt is much higher than a solution for wet spinning, the stretch ratio, defined by the ratio of the velocity of the filament at the take-up device to the average velocity of the melts at the exit of a spinnerette hole, is very high in melt spinning. Therefore one can control, to a certain extent, the physical properties of the finished fibers by judiciously choosing an optimum value of stretch ratio. This is because the stretch ratio can significantly affect the molecular orientation and crystallinity in the finished fiber.

In wet spinning, the polymer is dissolved in a suitable solvent and the solution is extruded through a spinnetette. The filaments thus produced are passed through a coagulating bath where the liquid threads just spun coagulate, giving solid filaments. The solvent originally put in the spin dope should be removed in the coagulating bath by the mechanism of counter-diffusion. Sometimes a chemical reaction also takes place in the coagulating bath (e. g. Viscose fiber, Acrylic fiber, Spandex (polyurethane) fiber, cellulose acetate and cellulos triacetate fiber, etc.). In contrast to the melt spinning process, the wet spinning process gives low stretch rate (hence low production rate) and low stretch ratio, which is mainly due to the large force acting on the filaments while passing through a liquid coagulating medium. There are some studies which showed how to determine the magnitude of the drag force in wet spinning [3].

In addition, the wet spinning process is economically less attractive than the melt spinning process, because an additional cost is involved in the removal of the solvent from the filaments spun. In general, more than one bath is needed to remove the solvent. Sometimes the steps involved with the after-treatment (washing and drying) are used for further stretching the filaments.

Dry spinning is usually recommended when the polymer has no definite melting point or is easily degradable when heated. In dry spinning, polymer solution is extruded through a spinnerette and the filaments spun are passed through a hot enclosed chamber through which a hot dry gas is passed. The solvent is evaporated from the filaments, leaving them solidified. As one may suppose, the dry spinning process calls for a solvent which has a low boiling point and a low heat of vaporization. In general, a non-polar solvent is preferred to a polar solvent. In addition, the solvent should meet the following requirements: ease of recovery, thermal stability, inertness, non-toxicity, minimum tendency to form electrostatic charges, and freedom from explosion hazard. Fibers dry spun are acrylic fiber and polyvinyl chloride fiber, etc.

From the point of view of solvent recovery, concentrated solutions are preferred for dry spinning. However, in practice, the preparation of concentrated polymer solutions is very difficult for two practical reasons, one is the solubility limit and the other is the difficulty in handling them. On the other hand, as in melt spinning, the dry spinning process can give a high stretch rate and hence a high production rate.

In recent years however, a new spinning technique has been introduced, which makes use of the combined features of either the dry-and wet-spinning or the dry-and melt-spinning methods. This spinning technique is called the air-gap spinning process. It has been developed primarily to take advantage of the good features of the individual processes (melt-,

wet-, and dry-spinning) for a given fiber-forming material, which otherwise would give either a poor fiber in its physical properties or a poor performance in its productivity.

There are two other recent developments in fiber spinning technique, which are worth mentioning. One is the production of the so-called shaped fibers, and another is the production of conjugate (or bicomponent) fibers. A shaped fiber is one whose cross section is non-circular. The formation of a conjugate fiber requires a means of producing a fiber consisting of two different components, extruded side by side. Each of these fibers has its advantage over the fibers spun by the conventional way.

In view of our interest in a better understanding of the fiber formation mechanisms, we shall review below some recent advances in synthetic fiber spinning. Since the subject is rather broad, it should be understood that the review presented below in a limited space is not exhaustive, and that many of the illustrations presented in the paper are taken from the research work of this writer, carried out during the past five years. Nevertheless it is earnestly hoped that readers will grasp some of the essential features of recent developments in synthetic fiber spinning.

2. Melt Spinning

Among the different processes (dry-, melt-, and wet-spinning) of producing man-made fibers, melt-spinning has been most extensively studied because it is relatively simple to treat both theoretically and experimentally, compared to the other two. However, a clear understanding of the phenomena occurring in the melt-spinning process is far from complete. The difficulty lies mainly in that, although one may be primarily interested in the fiber-forming step where stretching and reorientation of molecules occur, this step is governed to a large extent by the steps which precede it: namely, the deformation of the polymer melt in the spinnerette holes, and the relaxation of stresses in the melt upon exiting from the spinnerette.

It is a well-established fact that when a polymer melt exits from the spinnerette, it swells and gives rise to a maximum thread diameter at a short distance from the spinnerette face. Given a material, the exact location at which the maximum swelling occurs and the maximum thread diameter itself depend on the deformation history of the melt in the spinnerette holes.

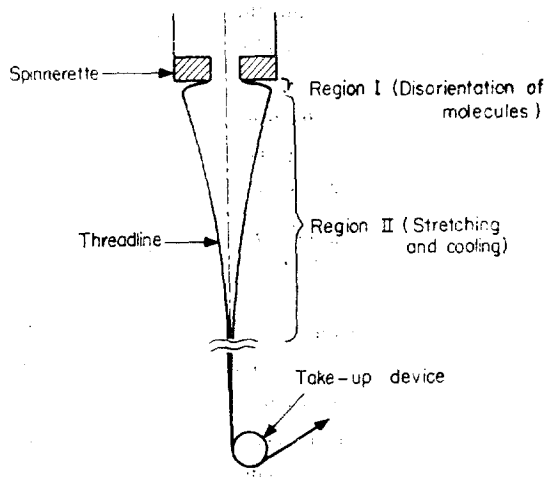

Fig. 1 Schematic diagram of a melt spun threadline under tension.

Consider a molten threadline being pushed out of a spinnerette hole and then being stretched by a take-up device. Referring to Figure 1, the molecules which were once oriented inside the spinnerette holes begin to disorient themselves upon exiting from the spinnerette in a very short distance from the spinnerette face. The orientation of molecules starts again under the influence of an axial velocity gradient (stretching). It may be supposed that molecular orientation ceases at a point where solidification of the molten threadline has progressed to such an extent, that the long molecular chains lose their mobility. We shall refer below to the region where molecular disorientation prevails as Region 1, and to the region where molecular reorientation prevails as Region 2.

A rigorous analysis of the flow behavior of a molten threadline in Region 1 is very difficult, if not impossible. For the purpose of analysis, the difficulty is compounded by the usually complicated expressio-

ns in the constitutive equations for viscoelastic fluids.

On the other hand, much effort has been spent on achieving a better understanding of flow problems in Region 2. which may be rather easily defined by making a few plausible, simplifying assumptions. To analytically treat the flow of polymer melts in Region 2, one needs to consider both the momentum transport in a moving threadline and the energy transport between the moving threadline and the coolant.

2.1 Rheological Properties Involved in Fiber Spinning

A fundamental rheological property which is important to fiber spinning is elongational viscosity, η_E, that may be defined as

$$\eta_E = \frac{F_{rheo}/A(x)}{\frac{dv(x)}{dx}} = \frac{S_{xx}}{\frac{dv(x)}{dx}} \qquad (1)$$

where F_{rheo} is the force required only for the deformation of the thread, $A(x)$ is the cross-sectional area of a thread at the position x, and $\frac{dv(x)}{dx}$ is the axial velocity gradient, sometimes called the elongation rate, of a thread under stretching. In the past, a number of investigators have attempted at experimentally determining the elongational viscosity by means of the melt spinning process [4,5,6,7,8] and by means of the wet spinning process[9,10].

As may be seen from Eq. (1), the determination of elongational viscosity involves measurements of F_{rheo}, $A(x)$, and $\frac{dv(x)}{dx}$. However, under a well-controlled experimental condition (e.g. isothermal melt spinning) measurements of the thread diameter, $D(x)$, alone will be sufficient to determine both $A(x)$ and $\frac{dv(x)}{dx}$ [4,5]. Of course F_{rheo} in Eq. (1) should be determined independently. Since elongational viscosity should be related to the molecular structure of polymers and further to the question of fiber "spinnability", we shall discuss below very briefly a means of determining the elongational viscosity experimentally.

Under some simplifying assumptions [7,10] one can write down the force balance equation

$$F_{rheo} = F_L + F_{grav} - F_{drag} - F_{inert} \qquad (2)$$

for a steady liquid jet under axial tension, issuing from a spinneertte hole into a liquid or gas medium. In Eq. (1) F_{grav} is the gravitational force that may be calculated from

$$F_{grav}(x) = \int_x^L \rho g \frac{\pi}{4} D(x)^2 dx \qquad (3)$$

where ρ is the density of the fiber-forming fluid, L is the distance from the spinnerette face to the position where the tension is measured, g is the gravity, and $D(x)$ is the fiber diameter at the position x. F_{drag} is the drag force that may be calculated[1,2] from

$$F_{drag}(x) = 0.843\ (\rho^0/\rho)\, W\ V(x)\ (\pi\rho\nu^{0(L-x)}/W)^{0.915} \qquad (4)$$

where ρ^0 is the density of the surrounding medium, and ν^0 is the kinematic viscosity of the medium, W is the mass flow rate, and $V(x)$ is the fiber velocity at the position x. F_{inert} is the inertial force that may be calculated from

$$F_{inert}(x) = W(V_L - V(x)) \qquad (5)$$

where V_L is the fiber velocity at $x=L$.

It may be seen then from Eq. (2) that the determination of F_{rheo} requires measurements of not only the thread tension, but also either the thread diameter or thread velocity as a function of the position x. Note that when an **isothermal** spinning experiment is carried out, one has

$$V(x) = 4W/\pi\rho D(x)^2 \qquad (6)$$

which permits one to calculate $V(x)$ from the measurements of $D(x)$. As one may surmise, the measurement of $D(x)$ is much easier than that of $V(x)$

A few research groups [4,5] have recently reported measurements of the thread diameter in isothermal melt spinning experiments. Figure 2 gives some representative results reported by Han and Lamonte [5]. It is seen that thread diameter decreases with spinning way and with take-up velocity, and that thread velocity calculated by the use of Eq. (6) increases with spinning way. Having measured the thread diameter, Han and Lamonte also calculated the magnitude of the individual forces involved in Eq. (2). Tables 1 and 2 give some representative results. It is seen from Table 1 that at relatively

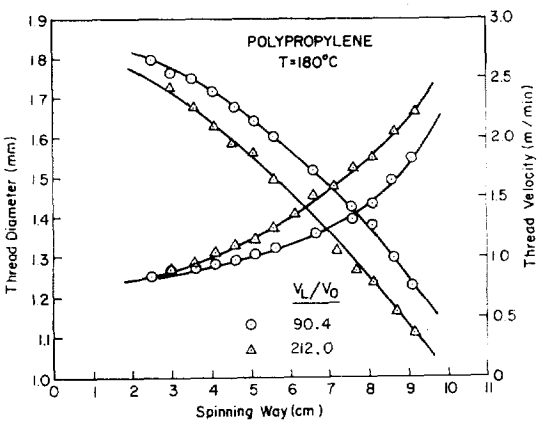

Fig. 2. Profiles of the thread diameter and thread velocity for polypropylene at 180°C ($Q = 1.606$ g/min; $V_o = 2.78$m/min.)

low stretch ratios the magnitude of F_{inert} is negligibly small compared to that of F_{grav} and F_{drag}, whereas as may be seen in Table 2 the magnitude of F_{inert} becomes as large as that of F_{drag}, which is due to the large stretch ratio (V_L/V_o=501.78).

Table 1. Force distributions in a low density polyethylene thread line

($W = 0.0247$ gms/sec; $V_O = 1.68$ cm/sec; $V_L/V_O = 22.28$; $T_O = 200$°C)

Distance (cm)	F_{grav} (gms)	F_{inert} (gms)	F_{drag} (gms)	F_{rheo} (gms)
1.0	0.0697	0.0000	0.0047	0.3474
3.0	0.0519	0.0000	0.0068	0.3274
5.0	0.0401	0.0001	0.0095	0.3132
7.0	0.0318	0.0002	0.0127	0.3034
9.0	0.0258	0.0002	0.0163	0.2970
12.5	0.0186	0.0004	0.0232	0.2924
17.5	0.0124	0.0007	0.0332	0.3025
22.5	0.0085	0.0016	0.0413	0.3200
25.0	0.0071	0.0022	0.0433	0.3324
27.0	0.0060	0.0030	0.0426	0.3461

Once F_{rheo} is determined one can proceed to calculate the elongational viscosity by use of Eq. (1). Figure 3 gives the recent results reported by Han and Lamonte[5], for four polymers investigated. It is seen that high density polyethylene, polypropylene, and polystyrene show a decrease in elongational viscosity as elongation rate is increased, and that,

Table 2. Force distributions in a polystyrene threadline

($W = 0.0455$ gms/sec; $V_O = 2.17$ cm/sec; $V_L/V_O = 501.78$; T_o-220°C)

Distance (cm)	F_{grav} (gms)	F_{inert} (gms)	F_{drag} (gms)	F_{rheo} (gms)
1.0	0.0811	0.0004	0.0063	2.8697
3.0	0.0398	0.0017	0.0172	2.8532
5.0	0.0212	0.0052	0.0419	2.8529
7.0	0.0122	0.0137	0.0902	2.8699
9.0	0.0075	0.0315	0.1741	2.9123
12.5	0.0037	0.1041	0.4423	3.0916
17.5	0.0017	0.3983	1.1500	3.7071
22.5	0.0008	1.2851	2.2515	5.2149
27.6	0.0005	3.6999	3.3731	7.8046
30.1	0.0004	5.8000	3.4594	9.3881

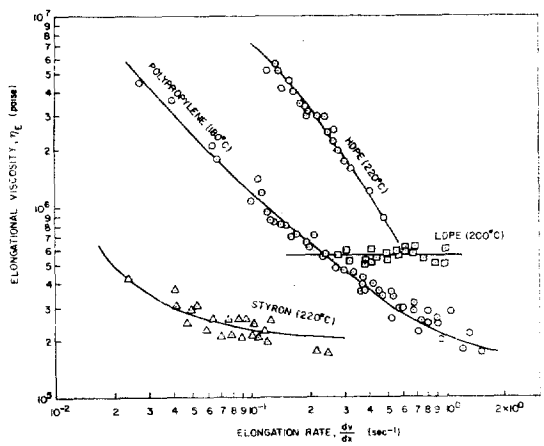

Fig. 3. Elongational viscosity versus elongation rate of polymer melts under isothermal spinning conditions.

on the other hand, low density polyethylene yields a constant elongational viscosity over the range of elongation rates investigated. This indicates that polymers having different molecular structures exhibit different rheological behavior in the elongational flow field. At present there appears to be no theory which could explain this experimentally observed fact.

2.2 Fiber Spinnability

In preparing polymers for manufacturing synthetic fibers, "spinnability" is of prime concern. Qualitatively, this term may be defined as the ability or ease of fiber formation under "normal" spinning conditions. It is generally understood that spinnability depends, among many other things, on (a) the rheological

properties of solutions or melts to be spun, (b) jet stretch, and (c) the rate of mass and heat transfer between the extruded filament and the medium. Here jet stretch is defined by the ratio of the velocity of the filament at the take-up device (V_L) to the average velocity of the melts (or solutions) at the exit of a spinnerette hole (V_o).

It is well known to the fiber industry that the thread breaks at a critical value of take-up velocity, V_L. This critical value depends on, among other things, the molecular structure, molecular weight, and molecular weight distribution. Often the maximum value of the jet stretch, $(V_L/V_o)_{max}$, has been used as a means of comparing the spinnability of differnt materials.

According to criterion, it can be said that the larger the value of $(V_L/V_O)_{max}$, the more spinnable a material is. This is because higher values of $(V_L/V_O)_{max}$ allow greater elongation of the thread without breaking. In their recent study [5], Han and Lamonte reported a plot of $(V_L/V_O)_{max}$ versus the number average molecular weight, $\bar{M}_n$, for the three high density polyethylenes investigated, which is given in Figure 4. According to these authors, the three polyethylenes used had almost constant values

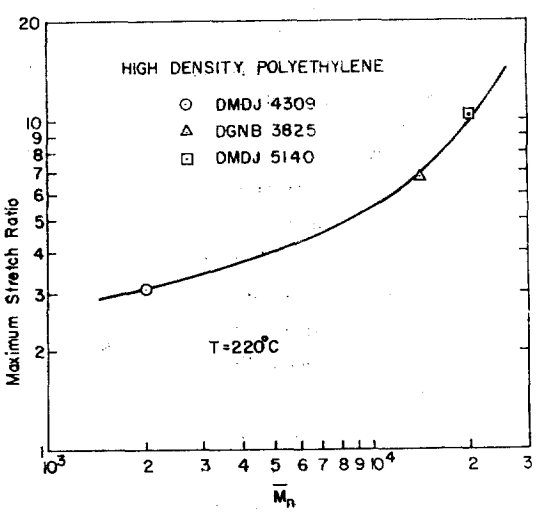

Fig. 4. Maximum stretch ratio versus number average molecular weight ($\bar{M}_n$) for three high density polyethylenes at 220°C.

of the weight average molecular weight, $\bar{M}_w$, the narrower the molecular weight distribution (i.e. the smaller the ratio of $\bar{M}_w$ to $\bar{M}_n$), the more spinnable a material is.

2.3 Molecular Orientation as Affected by Stretching

It has been a well-established fact that the mechanical properties of a finished fiber are strongly influenced by the orientation of molecules in the fiber. The extent of molecular orientation in the finished fiber may be controlled in two steps. One is in the spinning process itself, while the molten threadline gets stretched and cooled. The other is in the after-treatment process, where the already formed thread gets heated again and stretched.

The former is of greater importance, because in the fiber-forming step two structuring processes take place simultaneously: crystallization and molecular orientation. The orientation of molecules occurs in the direction of the axial velocity gradient, and hence the extent of molecular orientation depends on the elongation rate and also on the temperature profile along the spinning way. Because of the cooling effect, crystallization and orientation in melt spinning proceed in a highly complicated manner. When the crystallization rate is considerably lower than the rate of orientation, the macromolecules orient along the fiber axis, but form little crystalline regions. Hence, fibers spun from such polymers consist of amorphous, though axially-oriented molecules (e.g. polystyrene).

More than a decade ago, Ziabicki and his coworkers [11,12,13,14] made a pioneering investigation of the effect of spinning conditions on the orientation of molecules in melt spinning, both theoretically and experimentally. For the theoretical study, these authors considered the orientation of rigid ellipsoids and flexible coiled chains for the molecular segments in the elongational flow field and defined a "coefficient of orientation," which was suggested for use in determining the extent of orientation of macromolecules in melt spinning. And for the experimental study, measurements of fiber birefringence and x-ray patterns were made to correlate the orientation of macromolecules with spinning conditions and the molecular

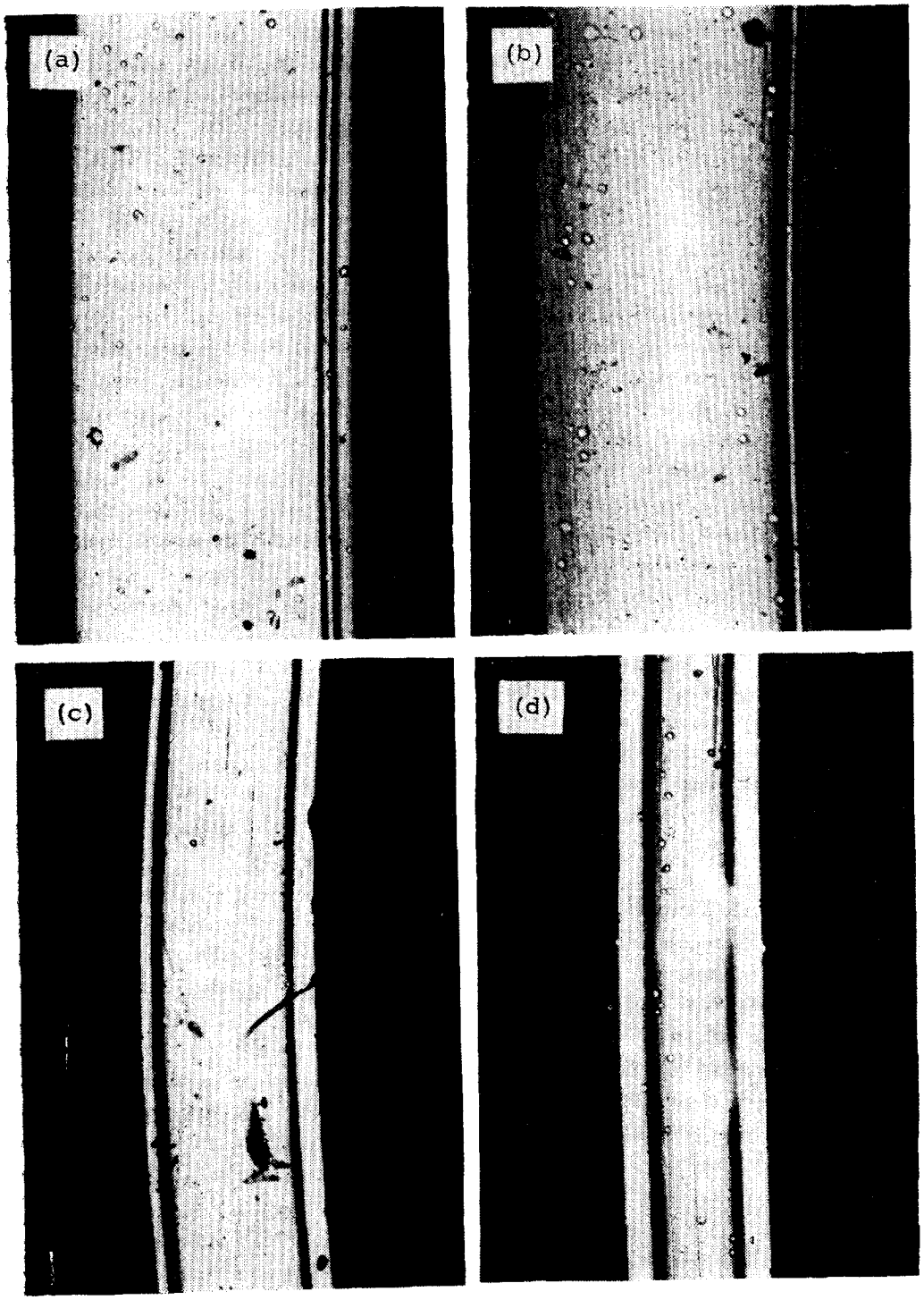

Fig. 5. Representative pictures of fiber birefringence of polypropylene monofilaments as seen through crossed pollarizers: (a) $V_L/V_o = 69$; (b) $V_LV/_o = 119$; (c) $V_L/V_o = 159$; (d) $V_L/V_o = 289$.

structure of the materials investigated.

On the other hand, Katayama [15] has measured the birefringence of a molten threadline along the spin line and has shown how much the stretching affects the orientation of molecules, which ultimately controls the mechanical properties of the finished filament. Other similar attempts are reported in a few recent contributions to the literature [16,17].

Recently, Han et al. [18] carried out an experimental study to investigate effects of stretch ratio on molecular orientation in polypropylene monofilaments, which were melt spun from a ribbon die into a water bath with adjustable air-gap distance between the two. By varying the air-gap distance and the rate of stretching, they obtained a variety of filaments of different molecular orientations. Figure 5 shows some representative pictures taken of birefringence (more specifically, retardation) in samples of ribbon fiber, which were collected under various stretching conditions[18]. Use of a ribbon die, instread of a circular die, has an advantage in that, when polarized light is passed through the sample there is very little edge effect on the birefringence measured with a very thin flat film. It is now seen from Figure 5, that retardation increases as the stretch rate is increased, indicating that the degree of orientation increases with stretch ratio.

Measurement of birefringence has long been used as a means of investigating orientation of molecules. Analysis of birefringence measurement with crystalline polymers, like the polypropylene, used in the study [18] of Han, is much more complicated than with amorphous polymers, such as polystyrene. This is because, in crystalline polymers, the crystalline phase becomes much more oriented than the amorphous phase when the polymer is stretched. This is one of the main reasons why much of the fundamental study has been made using polystyrene [19,20].

Since the stretching was uniaxial in the study by Han et al. [18], orientation of molecules would have occurred mostly in the direction of stretching. This is seen clearly from Figure 5, where interference fringes run parallel to the axis of the filament. Note also in Figure 5 that fringes are more closely spaced at the edges of the filament than at the center. This is attributable to the fact that cooling is faster at the edges of the filament than at the center, giving rise to different fringe orders (i. e. different orientations) across the filament width. That is, qualitatively speaking, fringe order (or retardation) increases regularly from zero to some maximum value going from the edge of the filament to the center, implying that more orientation of molecules would occur at the center than at the edge of the filament.

Although the relations between birefringence, orientation, and stress become much more complicated for crystalline polymers (e. g. polypropylene, polyethylene) compared to those for amorphous polymers, we can still qualitatively state that the degree of orientation in the ribbon samples of polypropylene tested is proportional to the amount of birefringence. Then, we can say from Figure 5 that the sample showing more fringes has a higher degree of orientation than the one showing fewer fringes. That is, the degree of molecular orientation increases with stretch ratio, which is as expected.

Of course, a quantitative investigation requires measurements of fringe orders, which is then to be related to stress distributions in a sample.

2.4 Heat Transfer Involved in the Melt Spinning Process

Cooling of threadline is very important in commercial melt spinning, and careful control of the rate of cooling of molten threadlines is very intimately related to producing a desired quality of finished fiber. The rate of cooling, together with the rate of stretching, influences both the degree of molecular orientation and the rate of crystallization.

Many of the previous studies therefore were concerned with certain aspects of the problems involved in melt spinning. Some [21,22,23] were concerned with the heat transfer between a moving threadline and the coolant; some [17,24,25] with molecular orientation in a filament as affected by various spinning conditions; others [4,5] with the deformation of a molten threadline spun into an isothermal chamber; and still others [26,27,28,29,30] with both deformation and heat transfer together.

Unfortunately, at present we do not have a clear understanding of the relationships between the rate of stretching and the degree of molecular orientation, and between it and the rate of cooling. Therefore a rigorous analysis of the melt spinning process is much more complicated than it may appear to be.

Referring to Figure 1, we shall consider Region 2, in which a molten threadline is stretched and cooled between the spinnerette and the take-up device. We can then write the following differential equations using cylindrical coordinates:

Equation of continuity:

$$\frac{1}{r}\frac{\partial}{\partial r}(\rho r v_r) + \frac{\partial}{\partial x}(\rho v_x) = 0 \tag{7}$$

r-component equation of motion:

$$\rho\left(v_r\frac{\partial v_r}{\partial r} + v_x\frac{\partial v_r}{\partial x}\right) = \frac{1}{r}\frac{\partial}{\partial r}(rS_{rr}) - \frac{S_{\theta\theta}}{r} + \frac{\partial S_{rx}}{\partial x} \tag{8}$$

x-component equation of motion:

$$\rho\left(v_r\frac{\partial v_x}{\partial r} + v_x\frac{\partial v_x}{\partial x}\right) = \rho g + \frac{1}{r}\frac{\partial}{\partial r}(rS_{rx}) + \frac{\partial S_{xx}}{\partial x} \tag{9}$$

Equation of energy:

$$\rho C_v\left(v_r\frac{\partial T}{\partial r} + v_x\frac{\partial T}{\partial x}\right) = -\frac{1}{r}\frac{\partial}{\partial r}(rq_r) - \frac{\partial q_x}{\partial x} + \left[S_{rr}\frac{\partial v_r}{\partial r} + S_{\theta\theta}\frac{v_r}{r} + S_{xx}\frac{\partial v_x}{\partial x} + S_{rx}\left(\frac{\partial v_x}{\partial r} + \frac{\partial v_x}{\partial x}\right)\right] \tag{10}$$

In Eqs. (7) to (10), S_{ij} are the ij-th components of stress; ρ is the fluid density; C_v is the heat capacity, g is the gravitational constant; q_r and q_x are the r-and x-components of heat flux, respectively; v_r and v_x are r-and x-components of velocity, respectively; and T is the fluid temperature.

If we now make the following simplifying assumptions: (a) V_x depends on x only, i. e. $v_x = v_x(x)$, (b) T depends on x only, i. e. $T = T(x)$, (c) q_x is negligibly small, (d) C_v is independent of T, (e) the viscous heat dissipation is negligible, which makes the bracketed term on the right-hand side of Eq. (10) drop out, then Eqs. (9) and (10) reduce to:

$$\rho v_x\frac{dv_x}{dx} = \rho g + \frac{1}{r}\frac{\partial}{\partial r}(rS_{rx}) + \frac{\partial S_{xx}}{\partial x} \tag{11}$$

$$\rho C_v v_x\frac{dT}{dx} = -\frac{1}{r}\frac{\partial}{\partial r}(rq_r) \tag{12}$$

We shall assume further that the following boundary conditions reasonably describe the physical situation under consideration:

(i) at $x = 0$, $v_x(0) = v_0$, $T(0) = T_0$ (13)

(ii) at $x = L$, $v_x(L) = V_L$ (14)

(iii) at $r = R(x)$, $q_r(R(x)) = h(T - T_a) + \lambda\varepsilon(T^4 - T_a^4)$ (15)

in which λ is the Stefan-Boltzman constant, and ε is the emissivity.

Now, multiplying both sides of Eq. (11) by $r\,dr$ and integrating the resulting equation from $r = 0$ to $r = R(x)$, we obtain:

$$\frac{\rho v_x R^2}{2}\frac{dv_x}{dx} = \rho g\frac{R^2(x)}{2} + R[S_{rx} - R'S_{xx}]_{r=R(x)} + \frac{d}{dx}\int_0^{R(x)} S_{xx} r\,dr \tag{16}$$

Where R' is the derivative of $R(x)$ with respect to x. Noting that the stresses at the surface $r = R(x)$ are given by:

$$[S_{rx} - R'S_{xx}]_{R=R(x)} = -F_d - 2H\sigma R' \tag{17}$$

in which F_d is the drag force, σ is the surface tension force, and H is the radius of curvature given by

$$H = \frac{1}{R[1 + (R')^2]^{3/2}} - \frac{R''}{[1 + (R')^2]^{3/2}} \tag{18}$$

Eq. (16) may be rewritten as:

$$\frac{1}{2}\rho v_x R^2\frac{dv_x}{dx} = \frac{1}{2}\rho g R^2 + R[-F_d - 2H\sigma R'] + \frac{d}{dx}\left[\frac{1}{2}S_{xx}R^2\right] \tag{19}$$

Again, multiplying both sides of Eq. (12) by $r\,dr$ and integrating the resulting equation from $r = 0$ to

$r=R$ gives:

$$\frac{1}{2}\rho C\ R^2\frac{dT}{dx}=-R\{h(T-T_a)+\lambda\varepsilon(T^4-T_a^4)\} \tag{20}$$

in which the boundary condition of Eq. (15) was used.

We can now further simplify Eqs. (19) and (20) by making use of the continuity condition:

$$Q=\rho\pi R^2V_x \tag{21}$$

where Q is the mass flow rate. Using Eq. (21) to eliminate R, Eqs. (19) and (20) reduce to:

$$v_x\frac{dv_x}{dx}=g+v_x\frac{d}{dx}\left(\frac{S_{xx}}{\rho v_x}\right)+2\sqrt{\frac{\pi v_x}{\rho Q}}\left\{-\ _d-2H\sigma R'\right\} \tag{22}$$

$$\frac{dT}{dx}=-\frac{2}{C_v}\sqrt{\frac{\pi}{\rho Q v_x}}\left\{h(T-T_a)+\lambda\varepsilon(T^4-T_a^4)\right\} \tag{23}$$

Equations (22) and (23) are general working equations whose solutions will describe the velocity and temperature profiles of a threadline along the spinway. It should be noted, however, that solution of Eqs. (22) and (23) requires the specification of S_{xx} in terms of the elongation rate $\frac{dv_x}{dx}$. Because a threadline gets cooled as it travels through the spinway, one needs an expression which shows how elongational viscosity varies as melt temperature is changed.

Very recently Han and Lamonte [5] have carried out isothermal melt spinning experiments at different melt temperatures, and they have found that the following semi-empirical equation holds for the observed elongational viscosity [30]:

$$\eta_E=3\alpha e^{\beta/T}\left[k_1+k_2\left(\frac{dv_x}{dx}\right)^{q-1}\right] \tag{24}$$

where

$$\alpha=\eta_0(T_0)e^{-E/RT_0}$$

$$\beta=E/R$$

$$E=E_s+E_e$$

Here E is the activation energy, determined experimentally, and consisting of two parts: one the shear flow activation energy E_s, which comes from the zero shear viscosity, and the other the elongational flow activation energy E_e. k_1 and k_2 are constants characteristic of the material being spun.

Han and Lamonte [30] have numerically solved Eqs. (22) and (23) with the aid of boundary conditions [13] and [14] and the semi-empirical expression, Eq. (24).

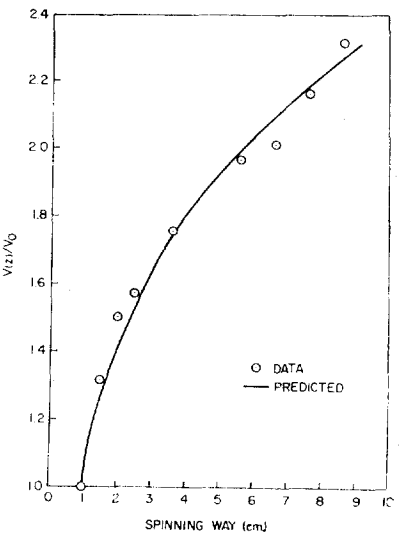

Fig. 6. Comparison of experimentally observed and theoretically predicted velocity profiles in polystyrene fibers. Spinning conditions: $Q=0.045$ g/sec; $V_0=2.17$ cm/sec; $V_0/V_L=501.7$; $T_0=220°C$; spinnerette diameter $=1.0$ mm.

Figure 6 gives representative results of the velocity profile in polyethylene fiber. Note that the solid line in Figure 6 represnts the theoretical prediction. Figure 7 gives predicted temperature profiles in fibers of polystyrene, low density polyethylene, and high density polyethylene. Note that these profiles are given just to demonstrate the reasonableness of the mathematical model developed. Note also that solution of Eqs. (22) and (23) enables one to evaluate the effect of individual heat transfer mechanisms involved in cooling the molten threadlines. It has been found that in melt spinning at high stretch ratios the effect of radiative heat transfer on the total heat loss while a filament is being stretched and cooled along the spinway, can be neglected, to all intents and purposes.

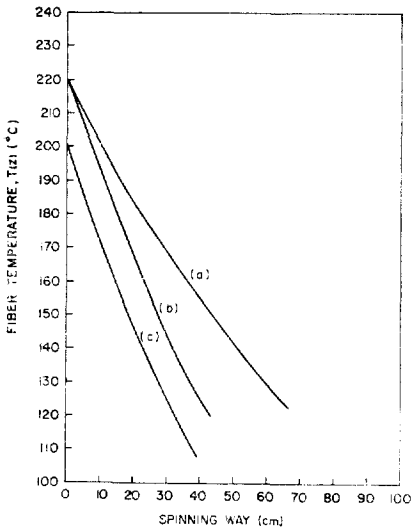

Fig. 7. Predicted temperature profiles in nonisothermal spinning: (a) high density polyethylene; (b) polystyrene; (c) low density polyethylene. Spinning conditions: $Q = 0.025$ g/sec; $T_o = 225°C$, $T_a = 25°C$.

3. Wet Spinning

In commercial wet spinning, a series of complex simultaneous operations are performed on and within each spun filament. These are: extrusion in the spinnerette hole (with associated shear stress generation and relaxation), fiber elongation, molecular orientation, coagulation, and crystallization. In addition, there occur counterdiffusion of solvent and nonsolvent between the solidified skin and fluid core [31,32] and counterdiffusion between the filament perimeter (coagulated skin) and coagulating bath [10,33]. Ignoring crystallization and heat transfer, a thorough investigation of this system would involve equations expressing mass transfer, the motion of threads being stretched, and the rheological behavior of the liquid thread in the elongational flow field. Furthermore, the physical constants needed to solve such a system of equations are very difficult to determine under such complex conditions. It is not surprising, therefore, that previous investigations have not dealt thoroughly with these aspects of the spinning process.

Recent work on the wet-spinning process itself has centered on the presentation of process parameters such as free diameter, jet stretch, or flow rate as functions of temperature, spinnerette hole size, etc. [31,32,33]. However, many of the more important correlations are not touched upon, probably owing to proprietary restrictions. Han [34] has recently attempted to correlate the rheological properties of spin dope with spinnability in the wet-spinning process.

3.1 The Effect of Coagulating Bath Conditions on Maximum Jet Stretch

It is clear that for a given throughput rate, the take-up velocity cannot be increased indefinitely. At a maximum take-up velocity, V_{2m}, the filaments begin to break in the bath at or near the face of the spinnerette. Spinning at this maximum velocity is just stable, since the continuous drawing of filaments cannot be realized above this critical value of take-up velocity. This maximum take-up velocity is a quantity depending on the spinning variables, such as the properties of spinning dope, composition and temperature of the coagulating bath, throughput rate, etc.

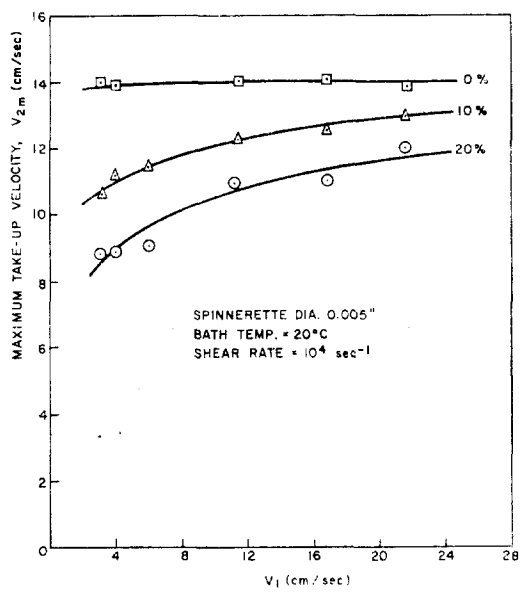

Fig. 8 Maximum take-up velocity versus throughput velocity. Spinnerette diameter = 0.005 in.; bath temp. = 20 °C; shear rate = 10^4 sec^{-1}.

Figure 8 shows plots of V_{2m} versus V_1 at various values of bath concentration. It is seen that below

20% bath concentration, the maximum take-up velocity decreases as the bath concentration increases. The maximum V_{2m} is attained at the condition of maximum coagulation rate, i.e., 0% bath concentration. In addition, the maximum take-up velocity V_{2m} is seen to increase as the throughput velocity increases. A similar result is reported by Paul [31]. Both of these results are in agreement with general expectations.

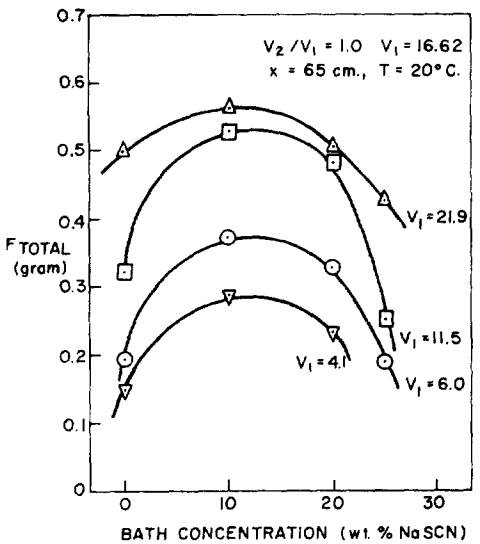

Fig. 9 Total tension versus bath concentration. V_2/V_1 = 1.0; x = 65cm; bath temp. = 20°C. Spin dope = 10% polyacrylonitrile (PAN.)

3.2 The Effect of Coagulating Bath Conditions on Tension

Figure 9 shows the effect of the bath concentration on the total measured tension at the takeup device (x = 60 cm) for a representative value of V_2/V_1. It is seen that all the curves behave in a similar manner. Note that the tensile force goes through a maximum for a bath concentration of about 10% NaSCN. This is extremely significant since it is known that commercial spinning is usually carried out with a comparable concentration of solvent in the coagulating bath (for this system). Undoubtedly the higher tension at this bath concentration increases spinnability and/or minimizes the possibility of thread breakage. Spinning under maximum tension, and therefore under maximum tensile stress, may also improve the tensile properties of the finished fiber by increasing molecular orientation in the preliminary (i.e., prewash) stages of the spinning process.

There are thus two apparent criteria for determining fiber spinnability. While filament tensions have a maximum at a bath concentration of 10%, the take-up velocity has a maximum at 0% NaSCN.

3.3 Spinnability and the Breakage Mechanism

Three factors which could affect spinnability and the mechanism of fiber breakage in the wet-spinning process may be isolated from the above discussions: (1) bath concentration; (2) system temperature; and (3) jet stretch. Bath concentration is important because this factor actually determines the rate of coagulation, skin formation, free velocity and maximum jet stretch, and tensile stress. Temperature is important primarily because it affects the structural viscosity of the spinning solution: the main effect of temperature is thus upon tensile stress and jet stretch rather than upon coagulation rate. Jet stretch is listed independently because it is actually a measure of the filament residence time in the bath; the larger the jet stretch, the shorter the filament residence time. Even under optimum conditions of temperature and concentration, the jet stretch may be considered to be an independent variable.

It has been stated that commercial spinning is performed under conditions of moderate bath concentration and at low temperatures. These conditions are probably close to optimum since solution viscosity, jet stretch, and coagulation rate are balanced so as to allow near-maximum tensions, near-maximum jet stretch, and probably the minimum chance of thread breakage.

At extremely low bath concentration, which brings rapid coagulation, the maximum tension attainable and the maximum jet stretch are both limited. This limitation may be caused by the breakage of the filament "skin," since at a very low bath concentration the rapid hardening causes formation of a solid skin which inhibits further coagulation of the fluid core [10,31,33]. The resultant breakage can be caused by "slippage" between the solid annular skin and the fluid core. Thus, this mechanism may be

more dependent on maximum take-up velocity V_{2m} than on tensile stress.

At somewhat higher bath concentrations, slower skin formation allows more thorough hardening of the entire fiber, and an optimum filament strength dependent on coagulation rate may be achievable. Breakage of the "slowly hardened" filament would then occur if a critical tensile stress is exceeded, and at this point the hardened portion would separate completely from the fluid (at or in the spinnerette) over the entire cross section of the filament.

It follows, therefore, that there is an optimum coagulation rate which is a function of bath temperature and concentration and which maximizes the combination of fluid and skin strength of the partially hardened fiber. Temperature may play a dual role here, since the effect of temperature on the dope viscosity appears to be more important than its effect on coagulation rate.

3.4 Mass Transfer Involved in the Wet Spinning Process

In the presence of hardening, the elongational viscosity depends not only on the rate of elongation, but also on the concentration of solvent in the elongating filament at constant temperature. The dependence of elongational viscosity on solvent concentration has not been studied hitherto, and therefore one may assume the following empirical expression:

$$\eta_E(dV/dx, C) = f(dV/dx)g(C).$$

That is, the effects of solvent concentration and rate of elongation on elongational viscosity can be separated. Elongational viscosity as a function of rate of elongation has been experimentally investigated and reported in a paper by Han [10]. The study indicates that elongational viscosity increases slightly with rate of elongation and then decreases slightly as the rate of eleongation approaches the maximum (near the breaking point of the filament). Furthermore, the study indicates that the influence of coagulation on the change of elongational viscosity is predominantly large compared to that of rate of elongation. Therefore, for all practical purposes, elongational viscosity may be assumed independent of rate of elongation, giving rise to the expression.

$$\eta_E(C) = 3\eta_0 g(C) \tag{26}$$

where $3\eta_0$ is the well-known Trouton viscosity [35].

Since the experimental data show that η_E increase with distance x in the elongating filament, $g(C)$ must be a function which relates the decreasing concentration of solvent in the filament to this increasing elongational viscosity. Physically, this concentration decrease is the cause of hardening (coagulation). The following expression for $g(C)$ is assumed based solely on the experimental results [33]:

$$g(C) = 1 + A[C_0 - C(x)] + B[C_0 - C(x)]^2 \tag{27}$$

where C_0 is the initial concentration of solvent in the dope on a polymer-free basis, $C(x)$ is the concentration of solvent in the elongating filament, and constants A and B are empirical constants to be determined. Thus, use of eqs. (26)-(27) in eq. (1) gives

$$V(x)\frac{dV(x)}{dx} = \frac{F_{theo}/Q}{3\eta_0\{1 + A[C_0 - C(x)] + B[C_0 - C(x)]^2\}} \tag{28}$$

which is to be solved for $V(x)$ as a function of x, with the boundary condition

$$V(x) = V_0 \text{ at } x = 0 \tag{29}$$

Here, V_0 is the velocity at the position of maximum jet swell, which is taken as the origin of our coordinate system. V_0 is determined from eq. (6) since the filament diameter at the position of maximum jet swell is photographically measured. However, in solving eq. (28) one has to know $C(x)$, the concentration profile of solvent, in the elongating filament along the spinning way. This necessitates solving a mass balance equation together with eq. (28). As noted above, a thorough investigation of the mass transfer process in wet spinning is a complicated matter. The refore, one may follow a less rigorous approach and take the mass transfer into account by

$$W\frac{dC(x)}{dx} = -K_m 2\pi R(x)[C(x) - C_b] \tag{30}$$

where W is the mass flow rate of dope, $C(x)$ is the weight fraction of solvent in the fiber (on a polymer-free basis), k_m is an overall mass transfer coefficient (g/sec cm²), $R(x)$ is the radius of the elongating filament, and C_b is the bath concentration of solvent. The assumptions made in formulating eq. (29) are: (1) a flat concentration profile within the filament at any position x; (2) a constant bath concentration, which is the equilibrium concentration of solvent in the filament.

Equation (30) may be rewritten by replacing $R(x)$ with $V(x)$ from eq. (6):

$$\frac{dC(x)}{dx} = \frac{-2k_m}{\rho}\sqrt{\frac{\pi}{Q}}\frac{C(x)-C_b}{\sqrt{V(x)}} \qquad (31)$$

where ρ is the density of filament. Equation (31) is to be solved for $C(x)$ with the boundary condition

$$C(x) = C_0 \text{ at } x = 0 \qquad (32)$$

where C_0 is the concentration of solvent in the dope on a polymer-free basis. This approach, though crude, will give some insight into the coagulation phenomenon, especially if the system is not overly sensitive to variations in A, B, and k_m.

The approximate concentration profiles of solvent, NaSCN, in the fiber was obtained by solving the mass balance equation, eq. (31), simultaneously with the force balance equation, eq. (28), the boundary conditions being given by eqs. (29) and (32).

The experiment simulated was one of very slow coagulation rate (33): bath concentration, 20% Na SCN; bath temperature, 20°C; spinnerette diameter, 0.015 in.; and V_2/V_f=1.95. The initial velocity V_0 was 12.7cm/sec, and the initial concentration C_0 was 0.484 g NaSCN/g spinning solution (polymer free).

Figure 10 shows plots of both the experimental and theoretical velocity profile for two sets of empirical constants, A and B. From eq. (31) it is seen that the concentration of solvent in the filament, $C(x)$, is dependent upon the square root of the filament velocity $V(x)$. Since $V(x)$ does not vary appreciably along the spinning way, $C(x)$ is not strongly dependent upon $V(x)$, or therefore upon parameters A and B. Thus, the given value of k_m

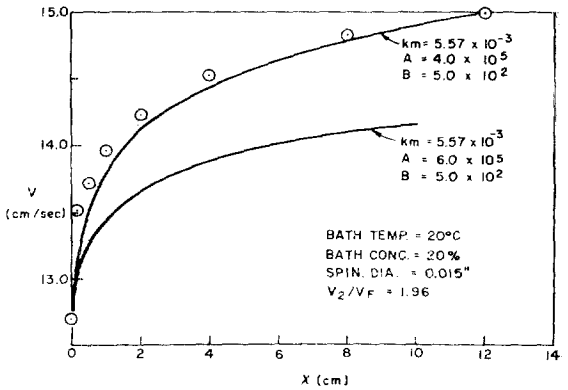

Fig. 10 Filament velocity versus spinning distance. V_2/V_f = 1.96; spinnerette diameter = 0.015 in.; bath temp. = 20°C; bath conc. = 20% NaSCN. Spin dope = 10% PAN.

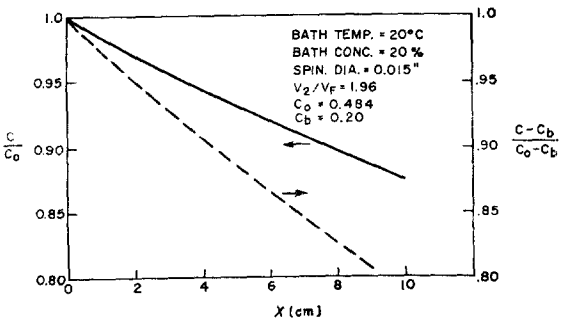

Fig. 11 Concentration profile of solvent in the filber. V_2/V_f = 1.96; spinnerette diameter = 0.015 in.; bath temp. = 20°C; bath conc. = 20% NaSCN; C_0 = 0.484; C_f = 0.20. Spin dope = 10% PAN.

is the best value for both sets of constants A and B given in Figure 10.

Figure 11 shows the resultant concentraton profile of solvent in the fiber. It must be borne in mind that this model is only a physical approximation and is most accurate over a short distance near the spinnerette, where appreciable thread deformation occurs.

From Figure 11 it is seen that approximately 94% of the original concentration of solvent remains in the filament at the distance of 4 cm from the spinnerette face. Since $C(x)$ can never go below the equilibrium (bath) concentration C_b, a measure of solvent removal with respect to the maximum amount of solvent which can be removed is $[C(x)-C_b]/(C_0-C_b)$. This quantity is also plotted in Figure 11, and it is seen that when 6% of the original solvent

is removed from the fiber, the solvent concentration has moved toward equilibrium by approximately 10%. By either measure, the percentage of solvent removed from the filament is very low. This is actually not surprising, since the concentration difference between the filament and the bath is very low. Furthermore, we are considering the average concentration in the filament at any position x.

At the surface of the filament, the concentration of solvent is, of course, very low, but this skin only accounts for a fraction of the total filament volume. It is clear from Figure 11 that most of the solvent must be removed from the filament in subsequent operations (washing), rather than during the coagulation and drawing step.

Lastly, it should be noted that the mass transfer mechanism postulated above does not hold true beyond a certain distance away from the spinnerette face, where the diffusion of solvent through a hard "skin" of the filament is a controlling mechanism. It should also be noted that essentially all of the thread deformation (i.e., elongation) occurs in a relatively short distance from the spinnerette face. Therefore, one can surmise that when there is not deformation in the spinning way, the force balance equation, eq. (28), loses its meaning, as does the mass balacne equation, eq. (31). Some authors [36] have made a study of mass transfer due to the diffusion mechanism for a spinning system similar to the one reported in this paper.

4. Dry Spinning

Dry spinning is the most complicated spinning technique of the three conventional spinning processes, and it has received the least attention of researchers from a fundamental point of view. This is mainly because an analysis of dry spinning process calls for the formulation of the system of three simultaneous equations, describing the momentum, energy- and mass-transfer. In the energy balance equation the term describing the latent heat of solvent vaporization, in addition to the term describing the convective heat transfer, must be included. And, in the mass balance equation the mechanisms of mass transfer should be included, describing 1) flash vaporization, 2) diffusion within the threadline, and 3) convective mass transfer from the threadline surface to the surrounding gas medium.

As one may suppose, the experimental determination of the physical constants associated with the mass and heat transfer, for instance the diffusion coefficient, heat and mass transfer coefficient, is very difficult in general. It can be then said that the lack of exprimental data has been a major reason why so little theoretical study has been carried out on dry spinning.

There are a few experimental studies reported on dry spinning in the recent literature [37,38,39]. However, much more experimental work needs to be done in order to better understand the complicated interactions, for instance, between the momentum- and mass-transfer, and between the mass- and heat-transfer. It is to be noted also that the elongational viscosity in dry spinning should be repesented in terms of the temperature and concentration, in addition to the stretch rate. This is because both the temperature and concentration keep changing while the fiber gets solidified along the spin line.

In view of the small amount of fundamental study reported in the literature on dry spinning, at present it is not possible to give a detailed review of the subject. Readers may consult with a recent review article by Corbiere [40].

5. Shaped Fiber Spinning

During the past decade the fiber industry has produced fibers having a variety of cross sections other than circular (so called "Shaped Fibers"), for instance elliptical and star-shaped fiberes[41,42]. What is most intriguing in making shaped fibers is that a desired shape of fiber can be produced from spinnerette holes, whose shape is quite different from that of the fiber itself. As may be surmised, there are many variables which may play an important role in the change of shape of a fiber's cross section.

For instance, it has been known to us that fibers

of an elliptical shape having various aspect ratios can be produced from the same rectangular spinnerette hole, by judiciously choosing spinning variables, such as jet stretch, bath concentration; etc. In addition, equally as important as, if not more important than the spinning variables are the rheological properties of the spin dope itself.

Because of the complexity of the problem a rigorous analysis of the processes involved in producing shaped fibers appears to have largely depended on trial and error. Hence, understandably much of the technology in this field has been kept as proprietary information by the various fiber manufactuers.

Recently Han [43] and Han and Park [44] have presented some interesting experimental observations, which were then used to explain why, for instance, an elliptical fiber can be produced from a rectangular spinnerette hole. Han [45] contended that wall normal stresses, distributed nonuniformly along the long and short sides of the rectangle, can give rise to a nonuniform swelling of extrudate upon its exiting from the spinnerette holes and hence possibly yield an elliptical fiber cross section. Han and Park [44] have undertaken an experimental program to investigate, by means of both wet-and melt-spinning, 1) the effect of shape and size of a spinnerette hole on the shape of extruded filaments, and 2) the effects of spinning conditions, such as jet stretch and bath concentration, on the shape of fibers spun. Representative results of their study will be discussed below.

There are three variables which may affect the fiber shape when spun through noncircular spinnerette holes. These are: 1) jet stretch, 2) coagulating bath concentration, and 3) throughput rate, Figure 12 gives pictures of fiber cross section spun through rectangular spinnerette holes having an aspect ratio of 3 into a water bath. It is seen that even a round fiber has been produced from a rectangular spinnerette hole. That is, the fiber shape does not resemble the spinnerette hole shape. Han and Park [44] report however that the resemblance increases as jet stretch increases.

They report further that the effect of jet stretch is

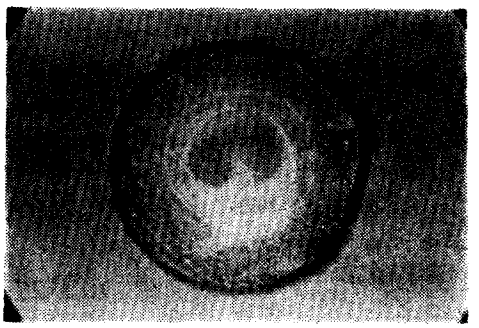

Fig. 12 Shape of fiber wet spun through rectangular holes having an aspect ratio of 3. Spin dope = 10% PAN.

not noticeable with the spinnerette having an aspect ratio of 3, whereas this was not the case with the spinnerette having an aspect ratio of 5 [44]. This then indicates that when a rectangular hole shape is used, a large aspect ratio is to be chosen in order to produce fibers resembling the spinnerette hole shape.

Therefore it may be said that, in order to produce shaped fibers with a rectangular spinnerette hole, a proper choice of aspect ratio is very important so that, at some reasonably high jet stretch, fiber shape can be maintained resembling the spinnerette hole shape. It should be noted, however, that a choice of too large an aspect ratio is rather detrimental to the process because, for a specified fiber denier, an increase in aspect ratio means a decrease in the dimension of the short side of the rectangular hole, which can lead to subsequent thread breakage even at some moderate value of jet stretch. Therefore there must be some optimum value of aspect ratio which would be most desirable from the processing point of view. Of course, such an optimum value would depend on the rheological properties of a spin dope, and to some extent it may depend on throughput rate, also.

Now, in the use of noncircular spinnerette holes, the swelling behavior of a spun fiber is more complicated than that in circular holes. As recently pointed out by Han [43], swelling of an extrudate from a rectangular hole, for instance, will be non-

uniform, giving rise to most swelling at the center of the long side of the rectangle. Han [43] has attributed it to the nonuniform distribution of wall normal stresses of a spin dope in the spinnerette hole. Han [43] also noted that, in wet spinning the surface tension force between the liquid thread being coagulated and the bath solution can be large enough to predominate over the normal stresses present in the liquid thread while it is being relaxed outside the spinnerette. When this happens, the fiber is still in the liquid state and tends to be circular due to the surface tension force. This appears, then, to explain the picture shown in Figure 12.

Note, on the other hand, that at a very high jet stretch the applied tension can be transmitted through the coagulated fiber in the bath to the liquid thread just outside the spinnerette face. In such an instance, the applied tension tends to overcome the surface tension force, giving rise to a fiber shape resembling the spinnerette hole shape more closely. This would then explain why fibers spun from the rectangular spinnerette having an aspect ratio of 3 are more round than those spun through the spinnerette having an aspect ratio of 5, because at a comparable jet stretch the smaller the aspect ratio, the more uniform the wall normall stresses would be and therefore the more readily the surface tension force can make the wet spun fibers round. Therefore it can be said that the surface tension force is prima-

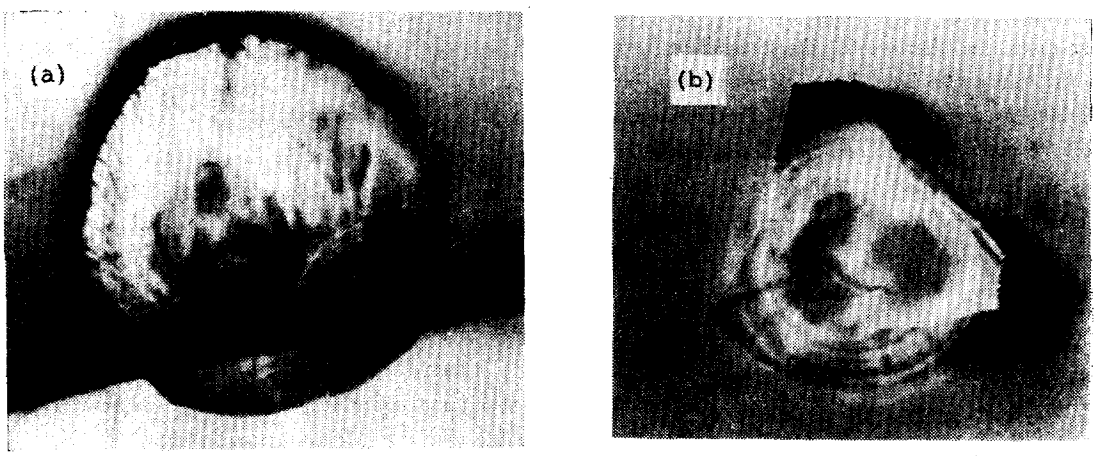

Fig. 13 Shape of fiber wet spun through trilobal holes: (a) bath conc. = 0% NaSCN (pure water), $V_L/V_o = 5.6$; (b) bath conc. = 0% NaSCN (pure water), $V_L/V_o = 10.5$. Spin dope = 10% PAN.

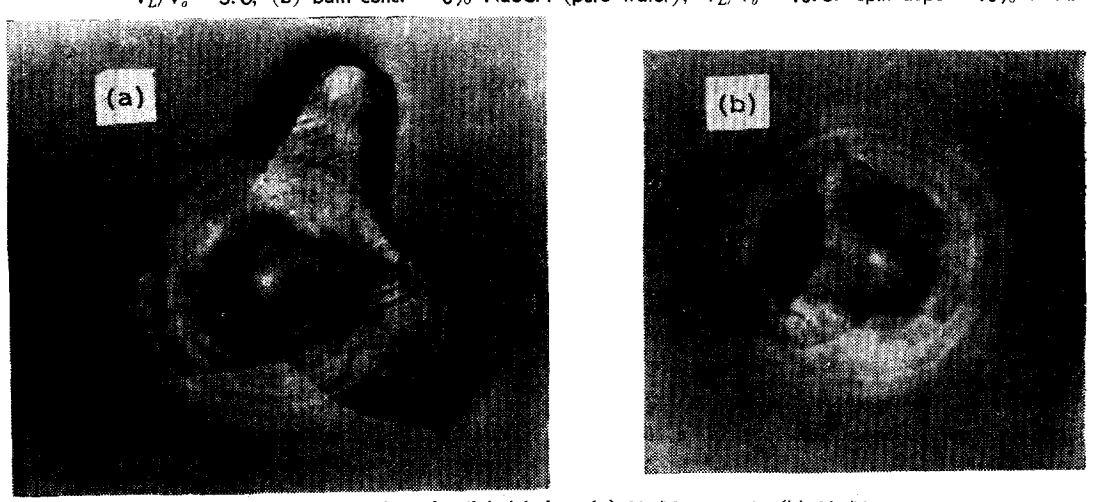

Fig. 14 Shape of fiber melt spun through trilobal holes: (a) $V_L/V_o = 10.6$; (b) $V_L/V_o = 30.5$

rily responsible for the roundness of the wet spun fiber.

When fibers were spun through trilobal holes and round holes with lugs, Han and Park [44] also found that the fiber shape also resembles the spinnerette hole shape more closely as jet stretch increases, being little influenced by the bath concentration. Some representative results are given in Figure 13 for fibers spun through trilobal holes, by means of the wet spinning. Some representative results of the polystyrene fiber shape are given in Figure 14 for fibers spun through trilobal holes, by means of the melt spinning. It is seen that, unlike in wet spinning, the fiber shape in melt spinning is little influenced by stretch rate, although the cross sectional area of the filaments gets smaller as the stretch rate is increased. In other words, the fiber shape resembles the spinnerette hole shape very much, being little influenced by stretch rate. Furthermore, it should be noted that the corners of the melt spun fibers are hardly rounded. This is attributable to the large values of the normal stresses predominating over the surface tension force, present in the molten filaments.

5. Conjugate Fiber Spinning

In manufacturing conjugate fibers, separate feed streams of polymer melts or solutions meet each other at the die inlet and then flow through spinnerette holes. As polymer melts or solutions possess both viscous and elastic properties, a theoretical analysis of the flow problems is much more complex than that of Newtonian fluids.

In recent years, there has been some important development reported on the production of conjugate fibers, which met some commercial success due to several industrial research groups, namely Sisson and Morehead [45] and Hicks et al. [46,47]. Sisson and Morehead[45] spun two viscose solutions side by side through circular spinnerette holes and successfully produced crimped fibers which possess a certain degree of bilateral structure in a rayon. Similarly, Hicks et al. [46] developed the bicomponent acrylic fiber ("Orlon" 21) which also produced crimps due to bilateral structure in an acrylic fiber.

An advantage of coextruding two components in a side-by-side semicircular configuration lies in that the technique can produce unique fiber properties which resemble natural wools, the so-called crimped fibers or wool fibers. The crimping characteristics result from the different thermal expansion coefficients of individual components, leading to the buckling of the filament while, upon exiting from the spinnerette it is either being cooled or coagulated along the length of the spin line.

It may be surmised that the distibution of the two components and their interfacial configuration in the molten state within a spinnerette hole is of paramount importance in ultimately controlling the amplitudes and frequencies of crimps in the solidified fiber. Despite the technological importance of this subject however, there seems to have been relatively little work reported in the literature on the fundamental nature of the flow characteristics of two viscoelastic polymer melts in circular dies.

A number of theoretical studies have been reported on the stratified flow of two immiscible Newtonian fluids in a circular tube. Gemmel and Eqstein [48] used a numerical technique to solve the equations of motion, and Bentwitch [49], and Yu and Sparrow [50] transformed the original system partial differential equations into a new set of equations in the complex plane.

These authors assumed that the interface between the components is smooth and ripple free, and that the effects of preferential wetting of the duct wall are negligible. It should be noted, however, that the theoretical analysis of polymer melt flow is much more complicated than that of Newtonian flow. It can indeed be said that previous attemps made at theoretically analyzing Newtonian fluids do not seem directly applicable to viscoelastic fluids.

Very recently, Southern and Ballman [51] made an interesting observation of the interfacial shape when two commercial polystyrenes were extruded through a circular hole (0.050 in. diameter and 3 in. leng-

th). Although these authors made an attempt to correlate the interfacial shape with the rheological properties (viscosity and elasticity) of the individual components in the molten state, their attempt has a few shortcomings due to insufficient data. First, there was no quantitative measurement taken of the flow properties of the bicomponent system while it was being extruded. Therefore it was not possible to evaluate, for instance, how much the pressure drop across the tube for a more viscous component is affected by the presence of a less viscous component. Second, the differences in die swell ratio between the two components were too small to be considered as an effective measure of the difference in their melt elasticities. That is, the die swell ratios of the individual components differed from each other only by 1~3%, which could be well within the measurement error.

Very recently Han [52] has made an interesting experimental study on bicomponent coextrusion through circular dies. For the study, two sets of two-phase systems were used, polystyrene/low density polyethylene, and polystyrene/high density polyethylene. The primary objectives of his study were (a) to investigate the effects of the viscous and elastic properties of individual components on flow behavior in the bicomponent coextrusion process, and (b) to investigate the shape of the inteface in the extrudate as affected by both the viscous and elastic properties of individual components.

Figure 15 shows pictures of the extrudate cross sections of the (a) low density polyethylene/polystyrene, and (b) high density polyethylene/polystyrene, coextruded through a die. It is seen that the high density polyethylene, which is more viscous and also more elastic than polystyrene, has a convex surface, whereas the polystyrene, which is more viscous and yet less elastic than the low density polyethylene, has a convex surface at the phase interface.

Now, in order to investigate the effects of viscous and elastic properties on the interfacial curvature, Figure 16 gives the melt viscosity versus shear stress,

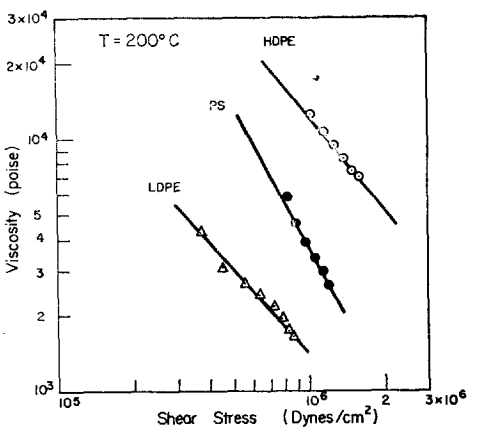

Fig. 16 Viscosity versus shear stress for polystyrene, low density polyethylene and high density polyethylene

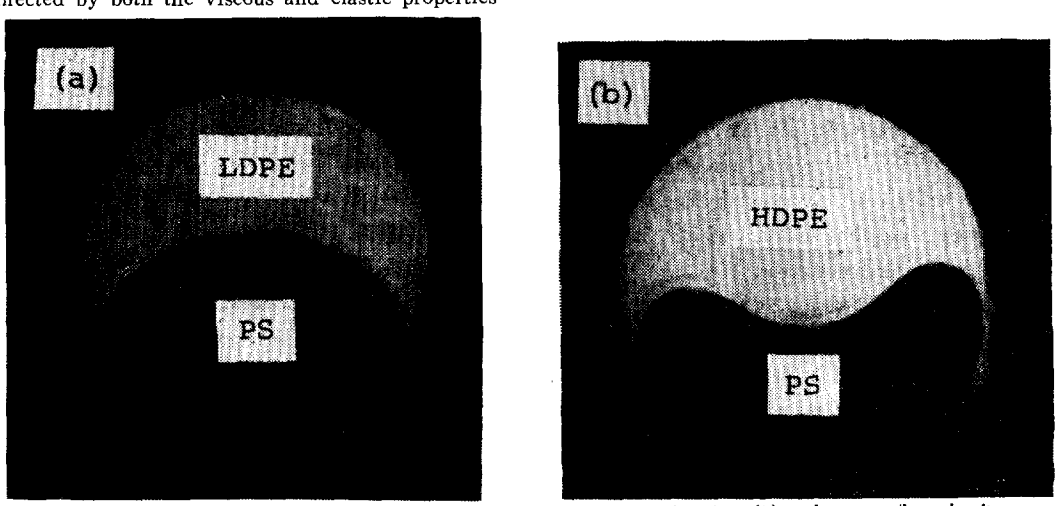

Fig. 15 Interface shape of the two-phase systems extruded through a circular die: (a) polystyrene/low density polyethylene (PS/LDPE) system; (b) polystyrene/high density polyethylene (PS/HDPE) system

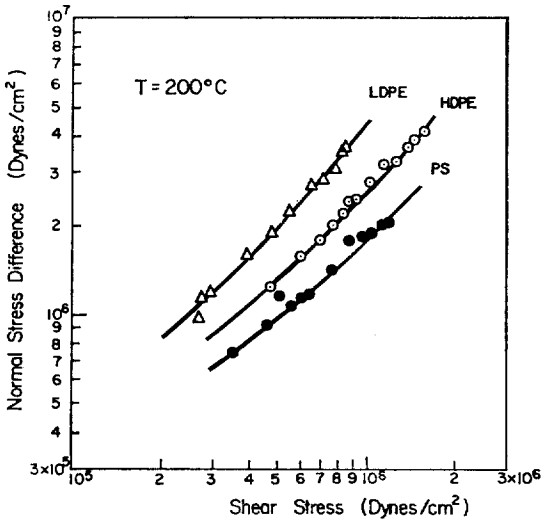

Fig. 17 Normal stress difference versus shear stress for polystyrene, low density polyethylene and high density polyethylene

and Figure 17 gives the normal stress difference versus shear stress, for the three materials extruded.

In view of his results, Han [52] concluded that whether or not a component tends to be convex or concave at the phase interface appears to be governed by the viscosity ratio and the two components involved. A similar conclusion has been drawn earlier by Southern and Ballman [51] who coextruded two commercial polystyrenes having different molecular weight distributions. In their study, however, die swell ratio was used as a measure of the elastic properties of the two polystyrenes used. Unfortunately, the die swell ratios of the two polystyrenes differed from each other only by 1~3%, which could as well be within measurement error. As may be seen from Figure 17, however, the normal stress differences of polystyrene and low density polyethylene differe from each other by more than 200%, which is beyond any possible measurement error.

What role then, if any, do the elastic properties of the two components involved play insofar as the interfacial curvature is concerned? Very recently, White et al. [53], using some simplifying assumptions, tried to determine theoretically the role which the elastic properties of two-phase viscoelastic fluids might play in determining interfacial curvature. Their analysis shows that the fluid with the greater second normal stress difference will tend to be convex into the other fluid. It should be noted, however, that the analysis is based on the assumption that the fluid viscosities in both phases are the same. Therefore it does not seem directly applicable to two phase systems which have widely different melt viscosities, as was the case in Han's study [52].

It should be noted, also, in Figure 15, that the phase interface is very smooth indeed (i.e. ripple free). It appears that the geometry of a die cross section might be a factor in the interfacial curvature of two phase systems. Han [52] speculated that the melt elasticity may be responsible for the occurrence of unstable (i.e. corrugated) phase interfaces.

References

1. B. C. Sakiadis, *AlChE J.*, **7**, 26(1961); *ibid.* 221 (1961); *ibid.* 467(1961).
2. A. B. Ziabicki, "Man-Made Fibers," vol. **1**, edited by H. Mark, S. M. Atlas and E. Cernia, Interscience Publishing Co., New York, 1967.
3. R. M. Griffith, *Ind. End. Chem. Fundam.* **3**, 245 (1964).
4. D. Acierno, J. N. Dalton, J. M. Rodriguez, and J. L. White, *J. Appl. Polym. Sci.*, **15**, 2395 (1971).
5. C. D. Han and R. R. Lamonte, *Trans. Soc. Rheol.*, **16**, 447(1972).
6. I. Chen, G. E. Hagler, L. E. Abbott, J. N. Dalton, D. C. Bogue, and J. L. White, *Trans. Soc. Rheol.*, **16**, 473 (1972).
7. A. Ziabicki, Kolloid-Z., **175**, 14(1961).
8. A. Ziabicki and K. Kedzierska, Kolloid-Z., **171**, 51 (1960).
9. M. Zidan, *Rheol. Acta*, **8**, 89(1969).
10. C. D. Han and L. Segal, *J. Appl. Polym. Sci.*, **14**, 2973(1970).
11. A. Ziabicki, *J. Appl. Polym. Sci.*, **2**, 24(1959).
12. A. Ziabicki and K. Kedzierska, *J. Appl. Polym. Sci.*, **2**, 14(1959).
13. A. Ziabicki and K. Kedzierska, *J. Appl. Polym. Sci.*, **6**, 111(1962).
14. A. Ziabicki and K. Kedzierska, *J. Appl. Polym.*

Sci., **6**, 361(1962).
15. K. Katayama, Paper presented at the 42nd Annual Meeting of the Society of Rheology, Knoxville, Tenn., October 1971.
16. T. Ishibashi, K. Aoki, and T. Ishii, *J. Appl. Polym. Sci.*, **14**, 1597(1970).
17. J. Furukawa, T. Kitc, S. Yamashita, and S. Ohya, *J. Polym. Sci.*, Part A-1, **9**, 299(1971).
18. C. D. Han, R. R. Lamonte, and L. H. Drexler, *J. Appl. Polym. Sci.*, in press(1973).
19. R. D. Andrews, *J. Appl. Phys.*, **25**, 1223(1954).
20. E. F. Gurnee, *J. Appl. Phys.*, **25**, 1232(1954).
21. T. R. Barnett, ACS preprints of Polymer Chemistry Division, p. 691, September 1966.
22. A. Ziabicki, *Appl. Polym. Symposia*, **6**, 2(1967).
23. E. H. Andrews, Brit. *J. Appl. Phys.*, **10**, 39 (1959)
24. T. Manabe, *J. Appl. Polym. Sci.*, **8**, 1097 (1964).
25. A. B. Thompson, Fiber Structure, Butterworths and The Textile Institute, Manchester and London, p. 480, 1963.
26. M. E. Morrison, *AIChE J.*, **16**, 57(1970).
27. S. Kase and T. Matsuo, *J. Polym. Sci.*, part A, **3**, 2541(1965).
28. S. Kase and T. Matsuo, *J. Appl. Polym. Sci.*, **11**, 251(1967).
29. O. L. Anderson, *J. Appl. Phys.*, **29**, 9(1958).
30. R. R. Lamonte and C. D. Han, *J. Appl. Polymer Sci.*, **16**, 3295(1972).
31. D. R. Paul, *J. Appl. Polylm. Sci.*, **12**, 2273 (1968).
32. D. R. Paul, *J. Appl. Polym. Sci.*, **12**, 383 (1968).
33. C. D. Han and L. Segal, *J. Appl. Polym. Sci.*, **14**, 2999(1970).
34. C. D. Han, Rheol. Acta, **9**, 355(1970).
35. F. T. Trouton, *Proc. Roy. Soc.* (London), **77**, 426(1906).
36. H. Takeda and A. Kato, Kogyo Tagaku Zasshi, **67**, 1285(1964).
37. Y. Sano and S. Nisikawa, *Kagaku Kogaku*, **30**, 245(1966).
38. Y. Ohzawa, Y. Nagano and T. Matsuo, Proc. 5th International Congress on Rheology, vol. 4, p. 393, Kyoto, Japan, October 1968.
39. Y. Ohzawa and Y. Nagano, *J. Appl. Polym. Sci.*, **14**, 1879, 1970).
40. J. Corbiere, "Man-Made Fiber," vol. 1, H. F. Mark, S. M. Atlas, E. Cernia, Eds., Interscience Publishing Co., New York, N. Y. (1967).
41. R. A. Buckley and *R. J. Philipps*, *Chem. Eng. Progr.*, **65**, No. 10, 41(1969).
42. R. C. Forney, L. K. McCune, N. C. Pierce, and R. Y. Tompson, *Chem. Eng. Progr.*, **62**, No. 3, 89(1966).
43. C. D. Han, *J. Appl. Polym. Sci.*, **15**, 1091 (1971).
44. C. D. Han and J. Y. Park, *J. Applied Polym. Sci.*, in press.
45. W. E. Sisson and F. F. Morehead, Textile Research J., **23**, 152(1953); *ibid.*, **30**, 153(1960).
46. E. M. Hicks, J. F. Ryan, R. B. Taylor and R. L. Tichenor, Textile Res. J., **30**, 675(1960).
47. E. M. Hicks, E. A. Tippets, J. V. Hewett, and R. H. Brand, "Man-Made Fibers," vol. **1**, edited by H. Mark, S. M. Atlas and E. Cernie, Interscience, N. Y., 1967.
48. A. R. Gemmel and N. Epstein, Can. *J. Chem. Eng.*, **40**, 215(1962).
49. M. Bentwich, ASME Trans.: *J. Basic Eng.*, **86**, 669(1964).
50. M. S. Yu and Sparrow, *AIChE J.*, **13**, 10(1967).
51. J. H. Southern and R. L. Ballman, paper presented at the 163rd ACS Annual Meeting, Boston, Mass., April 1972.
52. C. D. Han, *J. Appl. Polym. Sci.*, in press.
53. J. L. White, R. C. Ufford, K. R. Dharod, and R. L. Price, *J. Appl. Polym. Sci.*, **16**, 1313(1972).